AD_____

GRANT NUMBER DAMD17-94-J-4314

TITLE: Molecular Analysis of Motility in Metastatic Mammary Adenocarcinoma Cells

PRINCIPAL INVESTIGATOR: Jeffrey E. Segall, Ph.D.

CONTRACTING ORGANIZATION: Albert Einstein College of Medicine
of Yeshiva University
Bronx, New York 10461

REPORT DATE: September 1997

TYPE OF REPORT: Annual

PREPARED FOR: Commander
U.S. Army Medical Research and Materiel Command
Fort Detrick, Frederick, Maryland 21702-5012

REPORT DOCUMENTATION PAGE

Form Approved
OMB No. 0704-0188

1. AGENCY USE ONLY *(Leave blank)*	2. REPORT DATE	3. REPORT TYPE AND DATES COVERED
	September 1997	Annual (26 Aug 96 - 25 Aug 97)

4. TITLE AND SUBTITLE
Molecular Analysis of Motility in Metastatic Mammary Adenocarcinoma Cells

5. FUNDING NUMBERS
DAMD17-94-J-4314

6. AUTHOR(S)
Jeffrey E. Segall, Ph.D.

7. PERFORMING ORGANIZATION NAME(S) AND ADDRESS(ES)
Albert Einstein College of Medicine
of Yeshiva University
Bronx, New York 10461

8. PERFORMING ORGANIZATION REPORT NUMBER

9. SPONSORING/MONITORING AGENCY NAME(S) AND ADDRESS(ES)
Commander
U.S. Army Medical Research and Materiel Command
Fort Detrick, Frederick, Maryland 21702-5012

10. SPONSORING/MONITORING AGENCY REPORT NUMBER

11. SUPPLEMENTARY NOTES

12a. DISTRIBUTION / AVAILABILITY STATEMENT
Approved for public release; distribution unlimited

12b. DISTRIBUTION CODE

13. ABSTRACT *(Maximum 200)*

We report upon our studies (1) evaluating the relative roles of lamellipod extension and ruffling in metastatic behavior and (2) developing high resolution methods for localizing important cytoskeletal proteins to the leading edge of EGF-stimulated cells. (1) Addition of EGF or TGFα to metastatic MTLn3 cells results in the rapid extension of flat lamellipods. Nonmetastatic MTC cells do not express EGF receptor and show extensive ruffling in even in the absence of stimulation. Upon expression of the human EGF receptor in MTC cells, their metastatic ability is increased. In addition, stimulation of the EGF receptor results in transient suppression of ruffling and extension of lamellipods. We conclude that lamellipod extension, and not ruffling, is best correlated with metastatic ability. (2) In order to better identify proteins directly involved in stimulation of actin polymerization at the leading edge, we are developing methods for EM colocalization of newly polymerized actin with specific proteins with appropriate biochemical properties. Our preliminary results show highly improved resolution of the site of EGF-stimulated actin polymerization.

14. SUBJECT TERMS	15. NUMBER OF PAGES
Breast Cancer	32
	16. PRICE CODE

17. SECURITY CLASSIFICATION OF REPORT	18. SECURITY CLASSIFICATION OF THIS PAGE	19. SECURITY CLASSIFICATION OF ABSTRACT	20. LIMITATION OF ABSTRACT
Unclassified	Unclassified	Unclassified	Unlimited

FOREWORD

Opinions, interpretations, conclusions and recommendations are those of the author and are not necessarily endorsed by the U.S. Army.

___ Where copyrighted material is quoted, permission has been obtained to use such material.

___ Where material from documents designated for limited distribution is quoted, permission has been obtained to use the material.

___ Citations of commercial organizations and trade names in this report do not constitute an official Department of Army endorsement or approval of the products or services of these organizations.

___ In conducting research using animals, the investigator(s) adhered to the "Guide for the Care and Use of Laboratory Animals," prepared by the Committee on Care and Use of Laboratory Animals of the Institute of Laboratory Resources, National Research Council (NIH Publication No. 86-23, Revised 1985).

___ For the protection of human subjects, the investigator(s) adhered to policies of applicable Federal Law 45 CFR 46.

___ In conducting research utilizing recombinant DNA technology, the investigator(s) adhered to current guidelines promulgated by the National Institutes of Health.

___ In the conduct of research utilizing recombinant DNA, the investigator(s) adhered to the NIH Guidelines for Research Involving Recombinant DNA Molecules.

___ In the conduct of research involving hazardous organisms, the investigator(s) adhered to the CDC-NIH Guide for Biosafety in Microbiological and Biomedical Laboratories.

Jeffrey Clegall 11/20/87

PI / Signature Date

TABLE OF CONTENTS

Introduction

Chemotaxis plays an important role in many basic biological processes including embryogenesis, neurite growth, wound healing, inflammation and cancer metastasis. Studies with highly motile cells such as *Dictyostelium* (1), neutrophils (2) and platelets (3) in particular have shown that stimulation of cells with chemoattractant generates a transient increase in actin polymerization activity in the actin cytoskeleton. It is unclear how stimulation of cell surface receptors is linked to actin polymerization. Actin polymerization could be stimulated by severing or uncapping of pre-existing actin filaments, increasing availability of polymerization competent monomeric actin, or by de novo assembly of new filaments (1) (2).

EGF is a chemoattractant for MTLn3, a metastatic cell line derived from the 13762 NF rat mammary adenocarcinoma (4). We have described previously how MTLn3 cells rapidly extend F-actin filled lamellipods in response to stimulation with EGF(5). Lamellipod extension begins within 1 minute after addition of EGF and becomes maximal by 3 minutes after stimulation. Optimum lamellipod extension occurs at about 5 nM EGF, near the Kd of the binding of EGF to its receptor. Microchemotaxis chamber measurements also demonstrate that the chemotactic and chemokinetic responses of MTLN3 cells are greatest at 5 nM EGF(5). Actin polymerization is necessary for these EGF-stimulated responses because cytochalasin D inhibits the EGF-stimulated lamellipod extension, increases in F-actin in lamellipods, and chemotaxis in response to the addition of EGF. There is no significant change in the total F-actin content after a 3 minute stimulation with EGF compared to control cells, suggesting that either new actin polymerization was terminated by 3 minutes, that actin polymerization is exactly balanced by actin depolymerization or that actin polymerization was not involved in the EGF-stimulated redistribution of F-actin (5).

Well characterized chemoattractants for amoeboid phagocytes such as cAMP, fMLP and autocrine motility factor act through G-protein coupled receptors (6) (7) (8). However, chemoattractants for cells derived from mesenchymal and epithelial tissues, such as EGF, act through receptors that are receptor tyrosine kinases ((9) (10) (11) (12) and (13)). Most studies on EGF-stimulated signal transduction have been done on A431 cells (14) (15) and (16). Previous studies on EGF-induced reorganization of the actin cytoskeleton in A431 cells demonstrate the massive accumulation of F-actin and EGF-R in ruffles and under the plasma membrane at the free cell edge in colonies of A431 cells. F-actin content continues to increase with time after EGF addition in A431 cells (17) (14). Lipoxygenase and cycloxygenase products (15) but not phosphoinositide turnover (16) are involved in EGF-induced remodeling of the actin cytoskeleton in A431 cells. These results are consistent with the observation that the EGF-R is an actin binding protein den Hartigh et al, 1992) and that an EGF-R F- actin association may facilitate formation of a signaling complex containing other kinases and PLC γ in A431 cells (18).

Although A431 cells are useful for studies of signal transduction, A431 cells are neither highly metastatic nor motile and express abnormally high levels of EGF-R (19). MTLn3 cells on the other hand have high metastatic potential (20), are chemotactic to EGF (5) and the cell surface receptor for EGF is expressed at normal levels (21) (22). In addition, the motile and chemotactic responses of MTLn3 cells have similarities to those seen in well-characterized cells such as *Dictyostelium* and neutrophils (5). Thus MTLn3 cells provide a powerful model system for the study of EGF involvement in cell motility, metastasis and tumor cell chemotaxis. In addition, chemotactic responses to EGF may be particularly relevant to progression of breast cancer. Although the literature is mixed, there are reports that high expression of the EGF

receptor or its homologue HER2 (or ErbB2/neu) in breast cancers is correlated with poor prognosis. As presented in this report, we have utilized MTC cells expressing the human EGF receptor to demonstrate that EGF stimulates lamellipod extension and suppression of ruffling.

The relationship between chemoattractant-induced signal transduction and cortical actin reorganization is presently under intense investigation. The work presented in our previous report described our identification of the edges of the growing lamellipods as the sites at which EGF-stimulated actin polymerization is occurring. These are then the critical sites whose structure and composition must be understood in the hopes of identifying new proteins that could be targets for therapy or utilized as prognostic indicators in breast cancer. We also demonstrated that interaction with the substratum is not required for EGF-stimulated lamellipod extension, indicating that activation of cell-matrix receptors such as integrins is not necessary for EGF-stimulated actin polymerization. However, we found that talin, a protein that has been shown to nucleate actin filaments in vitro and is part of adhesion complexes in vivo, is localized at the sites of EGF-stimulated actin polymerization. Thus talin fulfills our criteria for a potential target and we are working further on talin as described below.

Additional significant effort has been necessary to get our analyses of the role of adhesion in lamellipod extension and the localization of the actin polymerization zones published. The localization of the polymerization zones is now accepted by the Journal of Cell Science. The analysis of the role of adhesion in extension is under revision for resubmission to Experimental Cell Research.

The research funded by grant DAMD17-94-J-4314 is focussed on identifying key proteins involved in regulation of cell motility and chemotaxis via the actin cytoskeleton. Based on the work described previously, cell-substratum adhesion molecules are not likely to

be critical for this. Other work indicates that actin filament capping proteins are also unlikely to be important for this process. We have identified talin as a strong candidate for stimulated actin nucleation, given that it has shown in vitro actin nucleation activity and is localized at the sites of actin nucleation (as determined by light microscopy). Thus for our final technical objective, we have focussed on altering the expression of talin in MTLn3 cells in order to evaluate its role in lamellipod extension and metastasis. For evaluation of other proteins that might be directly involved in control of actin polymerization during lamellipod extension, we are developing an electron microscope approach that provides much better spatial localization of proteins relative to sites of actin polymerization. This is important because colocalization at the light microscope level does not provide a clear separation between proteins that simply bind to actin filaments and proteins directly associated with the sites of actin polymerization.

Materials and Methods

Cell lines and culturing

The non-metastatic MTC line is a single cell clone from the parental tumor of the 13762NF rat mammary adenocarcinoma (4,20). MTC cells were transfected with retroviral expression vectors containing the human EGF receptor gene with a neomycin resistance gene (MTC HER 1/1) and a neomycin resistance gene alone as a transfection control (MTC neo) (23). They were grown in α-modified MEM containing L-Glutamine supplemented with 5% FCS and antibiotics. Cells were passaged as described (5).

Microchemotaxis chamber studies

Tissue culture dishes, Nucleopore filters, and glass coverslips were coated with 27 mg/ml rat tail collagen I in DPBS without calcium and magnesium for 2 h. For the analysis of chemotactic responses, a 48-well microchemotaxis chamber was utilized, essentially as described (5). During the 2 h collagen coating of a 8 um pore size Nucleopore filter, the cells were starved in α-modified MEM with 12 mM HEPES, pH 7.4 and .35 % BSA (designated MEMH). The appropriate chemoattractants in MEMH were placed in the lower chamber wells. The cells were harvested with 5 mM EDTA, pH 7.4 in DPBS, diluted to a density of 2×10^5 cells/ml in MEMH, and 50 ul were loaded into the upper wells in the chamber. After this point all steps were done as described previously(5).

Lamellipod extension assay

Cells were plated in 35 mm tissue culture dishes at a density of 25,000 cells/ml 18-24 h prior to experiment. The cells were serum starved in MEMH for 3 h prior to the addition of the appropriate dilution of TGFα. Cells were viewed using a Nikon Diaphot with a Nikon temperature chamber at 37° C. All area calculations and data reduction were done as described (5).

Scanning Electron Microscopy

Cells were plated onto coverslips 18-24 h prior to the experiment at a density of 25,000 cells/ml. Cells were serum starved for 3 h as above and stimulated with 5 nM TGFα in MEMH for 3 min. Cells were fixed in 2 % glutaraldahyde in Buffer F (137mM NaCl, 5 mM KCl, 1.1 mM Na_2HPO_4, 0.4 mM KH_2PO_4, 4 mM $NaHCO_3$, 5.5 mM glucose, 2 mM $MgCl_2$, 2 mM EGTA, 5 mM PIPES, pH 7.2) for 30 min. The cells were then rinsed in PBS, 3 x 5 min, and water, 3 x 5 min., and serially dehydrated in ethanol, from 30 to 100 %. They were then critical point dried and sputter coated for viewing. The cells were viewed in a JSM-6400 scanning electron microscope.

F-actin staining and quantitation

For F-actin staining, cells were plated onto coverslips at a density of 25,000 cells/ml 18-24 h before the experiment. They were starved as above for 3 h and stimulated with 5 nM TGFα for 0 (pre-stimulus),1, 2, or 3 min. Cells were fixed in Buffer F with 3.7% formaldehyde for 5 min and then permeabilized with 0.5% Triton X-100 in Buffer F for 20 min. After a 10 min rinse in 0.1 M glycine in Buffer F, and 5 rinses in TBS, the cells were incubated with 0.5 μM rhodamine phalloidin in TBS, pH 8.0 with 1 % BSA and 1% FCS for 20 min. The cells were then rinsed 6 x 5 min in TBS, pH 8.0 with 1 % BSA and mounted in 0.1 M N-propyl gallate, 0.02 % NaN_3, 50% glycerol in TBS, pH 8.0.

The cells were viewed using a N.A. 1.4 60x objective on an Olympus IX70. Data was collected using a cooled CCD camera manipulated with Oncor image 5.0 on a Macintosh 9500.

Quantitation of F-actin using the NBD-phallicidin assay was performed as described previously (24) with the following modifications. Cells ($2x10^5$) were plated 18 h before the beginning of the experiment. The cells were starved as above for 3 h and then stimulated with 5nM TGFα for 0 (pre-stimulation), 1, 2, 3 min. Cells were fixed and permeabilized with 3.7% formaldahyde and .5% Triton X-100 in Buffer F for 15 min. Cells were washed with PBS for 45 min and stained with 0.5 ml of 0.2 uM NBD-phallacidin in PBS for 1 h. Cells were washed with

PBS twice and the bound NBD-phallicidin was extracted using 0.5 ml 100% methanol for 90 min. Cells were washed twice and a BCA assay was performed at 37°C for 30 min to determine total cell protein in the sample. Fluorescence of the extraction solution for each sample was recorded at 465 nm excitation and 535 nm emission, and normalized against total cell protein. The experiment was also done by pre-treating the cells with 100 nM cytochalasin D in MEMH for 5 min prior to stimulation.

Electron Microscopy

MTLn3 cells were grown on Parlodion-carbon-coated gold square support grids on coverslips (Electron Microscopy Science, Fort Washington, PA) for 18-24 hours. The cells were starved for 3 hours in MEMH supplemented with 0.35 % BSA, and then stimulated with 5 nM EGF for 1 min. The coverslips were then treated with 0.25 % Triton X-100 in buffer C (138 mM KCl, 10nM Pipes pH 6.9, 0.1 mM ATP, 3mM EGTA ph6.9, 4mM $MgCl_2$) , 1% BSA and in the presence or absence of 0.45 uM G-actin for 1 min. After a rapid wash in buffer C, the preparations were fixed with 1% glutaraldehyde in cytoskeletal buffer pH 6-6.1 (5mM KCl, 137 mM NaCl, 4mM $NaHCO_3$, 0.4 mM KH_2PO_4, 1.1mM Na_2HPO_4, 2mM $MgCl_2$, 5mM Pipes, 2mM EGTA, 5.5 mM glucose) in the presence of 5 uM phallicidin for 15 min. The grids were then rinsed in cytoskeletal buffer and sequentially transferred through 4 drops of 40 ug/ml of bacitracin in water, followed by 4 drops of 1% phosphotungstic acid. The grids were then blotted dry and observed using a JEOL 100CX transmission electron microscope.

Results

Part 1: EGF stimulates lamellipod extension and inhibits ruffling

Chemotactic responses to TGFa are restored in MTC HER cells.

To assay whether expression of the human EGF receptor in MTC cells restored chemotaxis to TGFα, the microchemotaxis chamber assay was utilized. MTC cells do not show a chemotactic response to TGFα (5). In the presence of a gradient of TGFα, the number of MTC HER cells (MTC cells expressing the human EGF receptor) crossing the filter reached 9 times the number migrating towards buffer alone (Figure 1). A maximal chemotactic response was observed at 5 nM TGFα or above. MTC NEO cells (control transformed MTC cells) showed no increase in migration at any concentration of TGFα tested. For both MTC HER and MTLn3 cells, serum starvation increased the response to TGFα. MTLn3 cells under these conditions showed a response equal to 12 times over buffer alone (data not shown). Thus, expression of the human EGF receptor partially restored chemotactic responses to TGFα.

Lamellipod extension can be induced by TGFα in MTCHER cells..

To determine whether a restoration of TGFα-stimulated lamellipod extension paralleled the restoration of chemotactic responses, lamellipod extension induced by TGFα was measured as a change in cell area following stimulation. The parental MTC cells show no morphological changes, i.e. lamellipod extension or cessation of ruffling after TGFα stimulation (5). When cells were stimulated with TGFα, MTC HER cells showed an 18% increase in area 3 minutes after stimulation with TGFα (Figure 2). The amplitude of the response plateaued at concentrations of 1 nM TGFα and above. MTC NEO cells showed no response to TGFα at any concentration tested. MTLn3 cells show up to a 50% increase in area (Bailly et al., submitted).

Morphological changes induced by TGFα in MTCHER cells.

Morphologically, MTC, MTC NEO and MTC HER cells (in the presence or absence of serum) demonstrated an actively ruffling leading edge. Using scanning electron microscopy, this leading edge was clearly visualized as a series of 2 - 5 thin vertical sheets of membrane present within 5 um from the front of the cell (Figure 3A,B,E,F). MTLn3 cells show less concentrated ruffling at the leading edge, but strong ruffling over the entire dorsal surface (Figure 3 G). Observations of living cells were consistent with this: the leading edge of the MTC HER cell was phase dense and seen to continuously undergo alterations in size and shape, with forward protrusions often bending upwards to form vertical projections after lamellipod extension, while MTLn3 cells showed less extensive ruffling.

Upon stimulation with 5 nM TGFα, the leading edge flattened out in MTC HER cells, while it was unaffected in MTC NEO cells (Table 1 and Figure 3 C,D). Thus, stimulation with TGFα causes a cessation of ruffling at the time of maximal lamellipod extension. The percentage of MTC HER cells showing strong ruffling at the leading edge dropped from 92% to 26%, while the percentage of MTC NEO cells showing ruffling remained about 80 - 90% under all conditions. The reduction in ruffling was also seen for the MTLn3 cells, where the percentage of cells showing ruffling dropped from 96% to 12% (Table 1 and figure 3 G,H).

The ruffles showed a high concentration of filamentous actin, as demonstrated using staining with rhodamine phalloidin (Figure 4, 0 min). The vertical orientation of the ruffles results in bright staining with rhodamine phalloidin at the level of resolution of the light microscope. In MTC NEO cells, this staining remains constant after stimulation with TGFα. In MTC HER cells, however, the staining appears to redistribute into flatter lamellipod structures (Figure 4, 2 and 3min, Figure 3C, D). Ruffling resumes within 10 minutes of stimulation, concomitant with a reduction in area.

Changes in F actin in response to TGFα.

The changes in total filamentous actin (F-actin) that occur in MTC HER cells upon stimulation with EGF reflect a complex series of cytoskeletal changes that occur. To correlate

these behavioral changes with alterations in the polymerization state of actin, the amount of filamentous actin (F-actin) was assayed after stimulation (Figure 5a). In MTC HER cells, there is a peak in F-actin 2 minutes after stimulation, while MTC NEO cells show no increase in F-actin. Similar kinetics are seen for MTLn3 cells (Chan et al., submitted). In order to separate depolymerization of preexisting actin filaments from stimulation of new polymerization, depolymerization of F-actin was assayed by preincubating cells in 100 nM cytochalasin D. At this concentration , cytochalasin D blocks actin polymerization, chemotaxis and lamellipod extension without grossly altering cell morphology (5) over the time course of the experiment. Following stimulation with TGFα (Figure 5b), there is a stimulation of depolymerization beginning within 30 seconds and remaining for at least 5 minutes. Stimulation with TGFα in the presence of the carrier DMSO produces a normal increase in total Factin (data not shown). Thus TGFα stimulates both polymerization and depolymerization in MTC HER cells. Since the data in Figure 5a show the net effect of stimulated polymerization and depolymerization, while Figure 5b shows an estimate of the stimulated depolymerization, subtraction of 5b from 5a provides an estimate of the total stimulated polymerization of actin. This is shown in Figure 5c. There is a maximal polymerization after 2 minutes, followed by a sustained increase for at least 3 more minutes.

Part 2: Analysis of the role of talin in lamellipod extension

To directly test the function of talin in lamellipod extension, we have been evaluating antisense methods. We received a talin cDNA antisense expression vector from Dr. M. Block. The cDNA is in pMEP4, (Invitrogen). This vector utilizes an inducible metallothionein promoter to allow expression of proteins or RNAs that might be detrimental to cells (25). Cell were transformed with this vector and stable transformants identified. However, induction with cadmium did not lead to large reductions in talin content. We found at most a 20% reduction in total cellular talin, with no effects on cell morphology.

We have then subcloned the talin 5' cDNA into a second regulatable expression vector, pBPSTR-1. pBPSTR-1 utilizes a tetracycline-regulatable promoter. In the presence of tetracyclin, expression is suppressed. Removal of tetracyclin results in expression from the promoter. We have generated stable transformants and are now evaluating the talin expression levels upon induction of the expression of the antisense construct.

As an alternate approach to evaluating the function of talin the chemotaxis and metastasis of MTLn3 cells, we are collaborating with Dr. R. O. Hynes on expressing full length mouse talin in MTLn3 cells. Dr. Hynes has sent us the full length talin cDNA, and we are subcloning it into expression vectors in order to evaluate the effects of overexpression of talin on chemotaxis and metastasis.

Part 3: Development of a high resolution method for identifying proteins localized to sites of EGF-stimulated actin polymerization

An ever-expanding number of proteins can be localized to lamellipodia and ruffling membranes. Such a level of localization is to crude to provide meaningful information regarding the reason for localization to the lamellipod. The lamellipod can be considered as a subcellular organelle with a number of important properties - organization of adhesion sites, expression of matrix metalloproteases, structural reorganization of stress fibers, exclusion of microtubules, etc. Our interest is focused on the proteins directly involved in the stimulation of actin polymerization upon exposure to EGF. On the molecular level, the lamellipod is a large structure - 1 - 2 microns in width. Using either negative staining or rotary shadowing together with biotin labeled actin, we have found that the major site of EGF stimulated actin polymerization is localized to within about .2 um, directly at the edge of the lamellipod (Figures 6 and 7). This provides a method for directly testing the function of proteins that are localized to the lamellipod. Proteins directly involved in the stimulation of actin polymerization will be localized directly at the sites where biotin actin accumulates. Quantitation of protein localization compared to the sites of EGF-stimulated actin incorporation (Figure 8) will then allow a precise determination of the likelihood

of direct involvement in the stimulation of actin polymerization. Proteins which bind to actin after polymerization for other purposes, will not be found directly next to newly incorporated actin.

Discussion

In this report, we demonstrate that expression of the human EGF receptor in MTC cells is sufficient to restore chemotactic and other behavioral responses to TGFα. MTC cells and MTC NEO cells show little specific binding to EGF or TGFα, and upon stimulation with TGFα show none of the reported effects associated with such stimulation (5,21). The restoration of behavioral responses with expression of the human EGF receptor suggests that in these cells the machinery and signal transduction pathways involved in chemotactic responses are functional, and that with the expression of the appropriate receptor, the corresponding behavioral reactions can occur. Chemotactic responses and lamellipod extension in MTC HER cells showed roughly the same dose dependence as MTLn3 cells (5,26). However, the amplitudes of the responses in MTC HER cells do not match the responses of MTLn3 cells, ranging from 40 - 80% of the MTLn3 responses. This difference in amplitude could reflect subtle differences in the properties of the human EGF receptor compared to the rat EGF receptor, or reflect fundamental differences in the two cell types. In addition, this partial restoration of chemotactic responses in the MTC HER cells could explain the partial restoration of lung colonizing ability by those cells (23,27).

The general cycle of formation of ruffles in unstimulated MTC and MTLn3 cells - originating at the periphery of the cell, followed by movement along the dorsal surface towards the center is consistent with what has been observed with many cell types (28,29). Ruffles typically are formed from cell extensions which do not form a stable contact with the substratum and are then retracted. The detailed differences in this cycle between unstimulated MTC and MTLn3 cells was one property that was not affected by expression of the EGF receptor. The extensive ruffling that MTC cells demonstrate, seen as a series of ruffles moving back from the leading edge, but typically localized near the periphery, was still evident in both untransformed MTC cells and MTC cells transformed with control or EGF receptor expression constructs.

MTLn3 cells also showed ruffles moving back from the periphery, but they were less extensive and did not arrest at a particular site. Thus, this difference in ruffling activity is not solely due to a difference in expression of the EGF receptor. A number of other genes have been shown to be differentially expressed in MTC and MTLn3 cells (30). If these all reflect a single change in a master regulator gene, that master regulator gene is not the EGF receptor. Activation of the small G protein rac has also been shown to stimulate ruffling under certain conditions (e.g., (31)), and it is possible that the extensive ruffling seen in the MTC cell lines is due to constitutively activated rac. In that event, such constitutive activation is not sufficient to block responses to TGFα such as lamellipod extension, chemotaxis and actin polymerization.

The extensive ruffling present in the MTC cells provided an opportunity to clearly demonstrate that TGFα addition leads to the loss of ruffles as well as lamellipod extension. Both scanning electron microscopy and rhodamine phalloidin staining confirmed that 2 - 3 minutes after stimulation with TGFα, the degree of ruffling was reduced. This inhibition of ruffling is transient, and occurs during the time of prolonged lamellipod extension. Inhibition of ruffling after EGF stimulation was reported for the MTLn3 cells (5), but differs from what is seen with A431 cells (15,16,26,32,33), KB cells (34), and MCF-7 cells (35), which show increased ruffling. Indeed, NR6 cells show lamellipod retraction after stimulation (36). Since the MTC and MTLn3 cells are different clones from the same parental tumor, one possibility is that the response is dependent upon the cell type, and does not reflect species-specific differences in EGF receptor. An alternative possibility is that different expression levels of the EGF receptor result in different behavioral responses, with chemotactic responses, suppression of ruffling and lamellipod extension occurring at expression levels of about 50,000 per cell (as in the MTLn3 and MTC HER cells), and increased ruffling and reduced motility occurring at expression levels of 2 million receptors per cell (as in the A431 cells). Work is under way to vary the expression of the rat EGF receptor in MTC and MTLn3 cells to test this possibility.

At the cytoskeletal level, stimulation of MTC HER cells with TGFα leads to an increase in both depolymerization as well as polymerization of actin. F actin staining in ruffles is lost upon

EGF stimulation, and we propose that the depolymerization measured in whole cell extracts reflects the disappearance of ruffles, while the net polymerization reflects the stimulation of lamellipod extension via increased actin polymerization. This leads to a model for cell behavioral responses to the addition of TGFα, in which activation of the EGF receptor stimulates both lamellipod extension and ruffle breakdown, with the net result being formation of a new cell process in the direction of increased TGFα concentrations. Depending on the cell type or even the environment of a particular cell type, the balance between ruffling and lamellipod extension may be quite different. For example, at high confluence, the lack of available substratum for lamellipod extension or the presence of cell-cell contacts may lead to ruffling in response to stimulation of the EGF receptor, while at low confluence lamellipod extension might be the predominant response. The MTC cells are particularly convenient cells for studying this phenomenon, because they show very active ruffling. Although previous work with A431 cells has revealed EGF-stimulated polymerization and depolymerization, in those cells, polymerization correlated with cell rounding and depolymerization with removal of stress fibers (15). Thus, depending on the cell type which is under investigation, regulated depolymerization and polymerization of actin might result in quite different final cell behaviors.

For the MTLn3 and MTC cell lines, metastatic ability correlates with EGF-stimulated lamellipod extension and loss of ruffling. Such responses could contribute to metastasis by increasing cell motility as described by the three step model for metastasis (e.g.,(37)). For movement into new regions (away from the primary tumor or towards secondary sites), extension of a lamellipod from the front of the cell would lead to formation of new contact points. Disruption of old contact points at the rear of the cell followed by retraction of the rear would result in net cell movement in the direction of the extended lamellipod. Clearing of matrix from the front of the cell by matrix proteases would then provide new regions into cells could move by a new cycle of movement. In this model, suppression of unproductive cell extensions (ruffles) and stabilization of extended lamellipods would result in higher motility and, in turn, more efficient metastasis.

Conclusions

First, we have demonstrated that MTC cells expressing the human EGF receptor are chemotactic to TGFα (a ligand for the EGF receptor). Stimulation with TGFα also results in suppression of ruffling together with extension of actin-filled lamellipods. This demonstrates that ruffling and lamellipod extension are two separable phenomena, and that lamellipod extension is correlated with chemotactic responses. It is therefore important to distinguish between the effects of experimental manipulations on ruffling and lamellipod extension. In addition, because lamellipod extension is correlated with chemotactic responses (which are thought to be important for metastatic ability), the evaluation of lamellipod extension may have more relevance to evaluating the metastatic ability of cells.

Second, we have established a method for high resolution localization of specific proteins relative to the EGF-stimulated actin polymerization zone. This method will allow us to determine the location of specific proteins thought to be important for actin polymerization in order to evaluate their function in EGF-stimulated actin polymerization. Proteins that are closely associated with the polymerization zone will then be the focus for genetic manipulation to evaluate their role in metastasis and chemotaxis.

References

1. J. Condeelis, *Ann.Rev.Cell Biol.* **9**, 411 (1993).
2. S.H. Zigmond, *Curr.Opin.Cell Biol.* **8**, 66 (1996).
3. K. Barkalow, J.H. Hartwig, *Biochemical Society Transactions* **23**, 451 (1995).
4. A. Neri, D. Welch, T. Kawaguchi, G.L. Nicolson, *J.Natl.Cancer Inst.* **68**, 507 (1982).
5. J.E. Segall, *et al*, *Clin.Exp.Met.* **14**, 61 (1996).
6. P.N. Devreotes, S.H. Zigmond, *Annu.Rev.Cell Biol.* **4**, 649 (1988).
7. S. Silletti, A. Raz, *Biochemical & Biophysical Research Communications* **194**, 446 (1993).
8. M. Stracke, L.A. Liotta, E. Schiffmann, *Symposia of the Society for Experimental Biology* **47**, 197 (1993).
9. T. Hoelting, A.E. Siperstein, O.H. Clark, Q.Y. Duh, *Journal of Clinical Endocrinology & Metabolism* **79**, 401 (1994).
10. P.H. Pedersen, *et al*, *International Journal of Cancer* **56**, 255 (1994).
11. L.S. Royce, B.J. Baum, *Biochimica et Biophysica Acta* **1092**, 401 (1991).
12. G.R. Grotendorst, Y. Soma, K. Takehara, M. Charette, *Journal of Cellular Physiology* **139**, 617 (1989).
13. J. Blay, K.D. Brown, *Journal of Cellular Physiology* **124**, 107 (1985).
14. J. Boonstra, *et al*, *Cell Biology International* **19**, 413 (1995).
15. M.P. Peppelenbosch, L.G. Tertoolen, W.J. Hage, S.W. de Laat, *Cell* **74**, 565 (1993).
16. C.Y. Dadabay, E. Patton, J.A. Cooper, L.J. Pike, *J.Cell Biol.* **112**, 1151 (1991).
17. P.J. Rijken, W.J. Hage, P.M. van Bergen en Henegouwen, A.J. Verkleij, J. Boonstra, *J Cell Sci.* **100**, 491 (1991).
18. M. Diakonova, *et al*, *J Cell Sci.* **108**, 2499 (1995).
19. J.E. Price, D.N. Sauder, I.J. Fidler, *J.Invest.Dermatol.* **91**, 258 (1988).
20. D.R. Welch, A. Neri, G.L. Nicolson, *Inv.Met.* **3**, 65 (1983).
21. A.M. Kaufmann, *et al*, *Int.J.Oncol.* **4**, 1149 (1994).

22. R.B. Lichtner, *et al, J Biol.Chem.* **267**, 11872 (1992).

23. R.B. Lichtner, *et al, Oncogene* **10**, 1823 (1995).

24. J. Condeelis, A.L. Hall, *Methods Enzymol.* **196**, 486 (1991).

25. L. Tranqui, M.R. Block, *Experimental Cell Research* **217**, 149 (1995).

26. R.B. Lichtner, M. Wiedemuth, C. Noeske-Jungblut, V. Schirrmacher, *Clin.Exp.Met.* **11** , 113 (1993).

27. A.M. Kaufmann, R.B. Lichtner, V. Schirrmacher, K. Khazaie, *Oncogene* **13**, 2349 (1996).

28. T.J. Mitchison, L.P. Cramer, *Cell* **84**, 371 (1996).

29. J.P. Heath, B.F. Holifield, *Symposia of the Society for Experimental Biology* **47**, 35 (1993).

30. S.D. Pencil, Y. Toh, G.L. Nicolson, *Breast Canc.Res.Treat.* **25**, 165 (1993).

31. A.J. Ridley, *Bioessays* **16**, 321 (1994).

32. M. Chinkers, J.A. McKanna, S. Cohen, *J.Cell Biol.* **88**, 422 (1981).

33. M. Chinkers, J.A. McKanna, S. Cohen, *J.Cell Biol.* **83**, 260 (1979).

34. Y. Miyata, E. Nishida, H. Sakai, *Experimental Cell Research* **175**, 286 (1988).

35. N.A. van Larebeke, M.E. Bracke, M.M. Mareel, *Cytometry* **13**, 1 (1992).

36. J.B. Welsh, G.N. Gill, M.G. Rosenfeld, A. Wells, *J Cell Biol.* **114**, 533 (1991).

37. L.R. Bernstein, L.A. Liotta, *Current Opinion in Oncology* **6**, 106 (1994).

Table 1: Effect of TGFα stimulation on cell ruffling*

	unstimulated	5nM TGFα
MTC HER	92%	26%
MTC neo	88%	82%
MTLn3	96%	12%

* Data are presented as the percent of cells with leading edge ruffling before and 3 min after TGFα stimulation in MTC HER , MTC NEO and MTLn3 cells. Total cells counted for each condition is 50.

Figure Legends

Figure 1: Migration of MTC HER (squares) and MTC NEO cells (circles) in response to TGFα. For each experiment, the number of cells crossing the filter in 3 h was normalized to the average number crossing in the absence of TGFα (average value 40). These normalized values were averaged for ensemble mean and SEM for a total of 12 wells in three separate experiments. TGFα was present in the bottom well only.

Figure 2: Sensitivity of lamellipod extension of MTC HER cells (squares) and MTC NEO cells (circles) to TGFα. The area of each cell relative to the prestimulus area was determined 3 min after stimulation with TGFα. These normalized values were averaged for each cell line to produce a mean and SEM. Each data point represents the mean of 24 -30 cells from 3 experiments.

Figure 3: Scanning electron micrographs of unstimulated (A,B) and TGFα- stimulated (C,D) MTC HER and unstimulated (E) and stimulated (F) MTC NEO cells and unstimulated (G) and stimulated (H) MTLn3 cells. B and D are higher magnification views of the leading edges of the cells in A and B. In the unstimulated MTC HER cells, the leading edge shows active ruffling, while 3 min after TGFα stimulation, the MTC HER leading edge completely flattens out. In the MTC NEO cells no change in ruffling is seen after stimulation. The unstimulated MTLn3 cells show active ruffling over the entire dorsal surface that becomes completely flattened out 3 min after stimulation.

Figure 4: Localization of F-actin using rhodamine phallodin in MTC HER and MTC NEO cells stimulated with TGFα. The brightly staining ruffles at the leading edge of the MTC HER cells are gone by 2 min and the cells are completely flattened by 3 min, showing staining for F-actin at the leading edge of the lamellipod. MTC NEO cells show no morphological changes after TGFα stimulation. Scale bar = 20 μm.

Figure 5 Changes in F-actin after stimulation with TGFα. (A): Total F-actin associated with MTC HER (squares) and MTC NEO (circles) cells after TGFα stimulation and MTC HER cells stimulated with buffer alone (triangles). (B) After preincubation with 100 nM cytochalasin D to block polymerization, TGFα–stimulated depolymerization of F actin was measured in MTC HER cells. MTCHER cells were stimulated with TGFα (squares) or buffer (triangles). (C) Estimated total actin polymerization. The data in figure 5B were subtracted from the data in Figure 5A to estimate the total polymerization occurring in the absence of depolymerization.

Figure 6. Incorporation of biotin labeled actin into MTLn3 cells stimulated with EGF. MTLn3 cells were stimulated with EGF for 0 (A), .5 min (B), 1 min (C), and 3 min (D), then permeabilized in the presence of biotin labeled actin as described in Materials and Methods. The cells were then labeled with 5 nm gold anti-biotin (small dots) and 15 nm anti-talin (larger dots).

Figure 7. Stereo pair images from a quick frozen, rotary shadowed cell 3 min after stimulation . MTLn3 cells were stimulated with EGF for 3 min, then permeabilized in the presence of biotin labeled actin as described in Materials and Methods. The cells were then labeled with 5 nm gold anti-biotin.

Figure 8. Quantitation of incorporation of biotin labeled actin following EGF stimulation. (A) The number of small gold particles indicating incorporated biotin actin was quantitated as a function of distance from the leading edge (LE). (B) The filament density was quantitated as a function of distance from the leading edge.

Figure 1: TGFalpha Chemotaxis

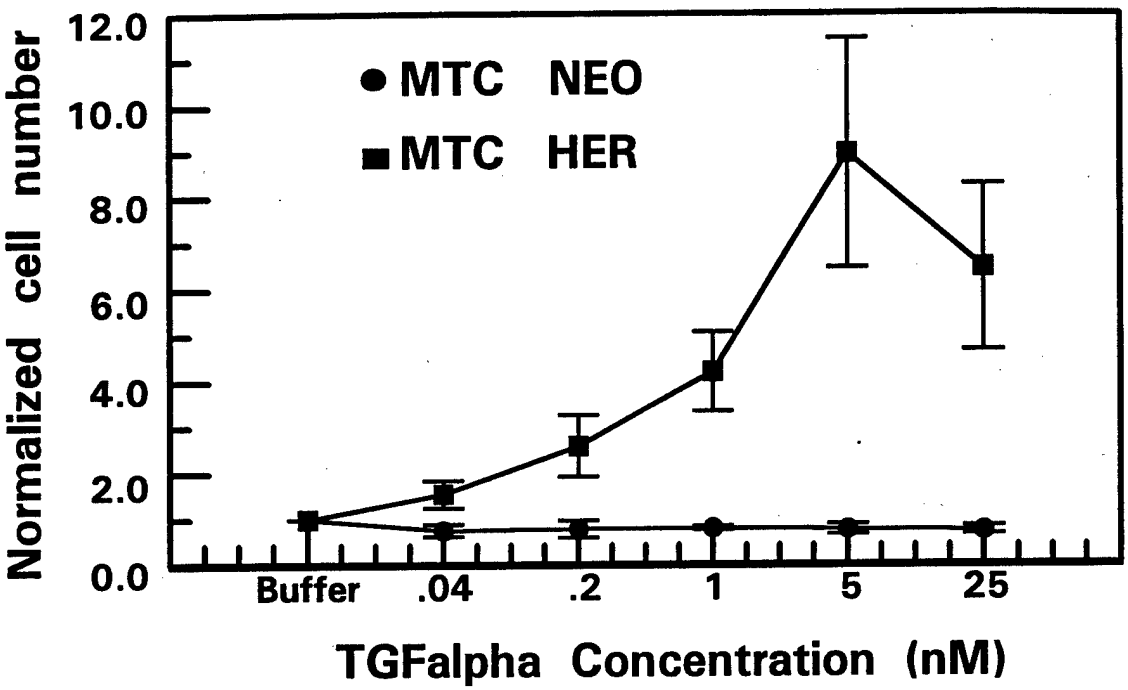

Figure 2: Lamellipod Extension

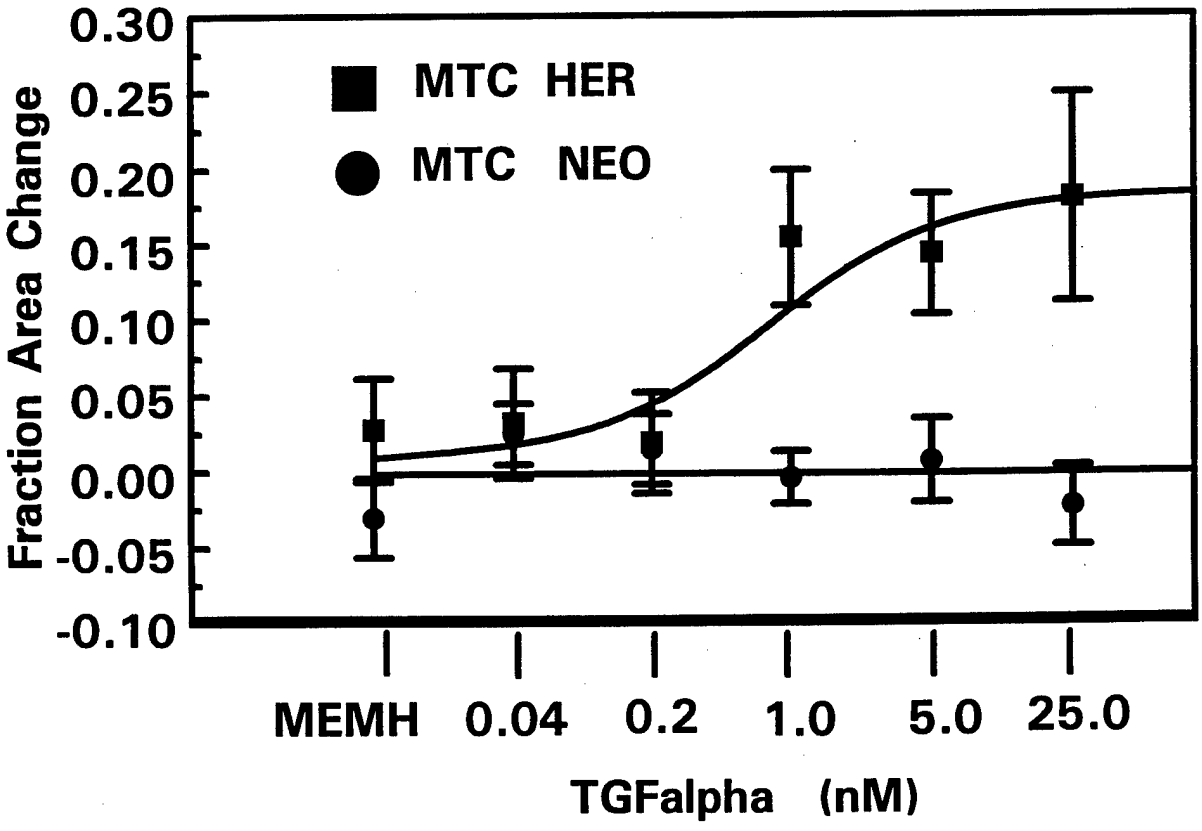

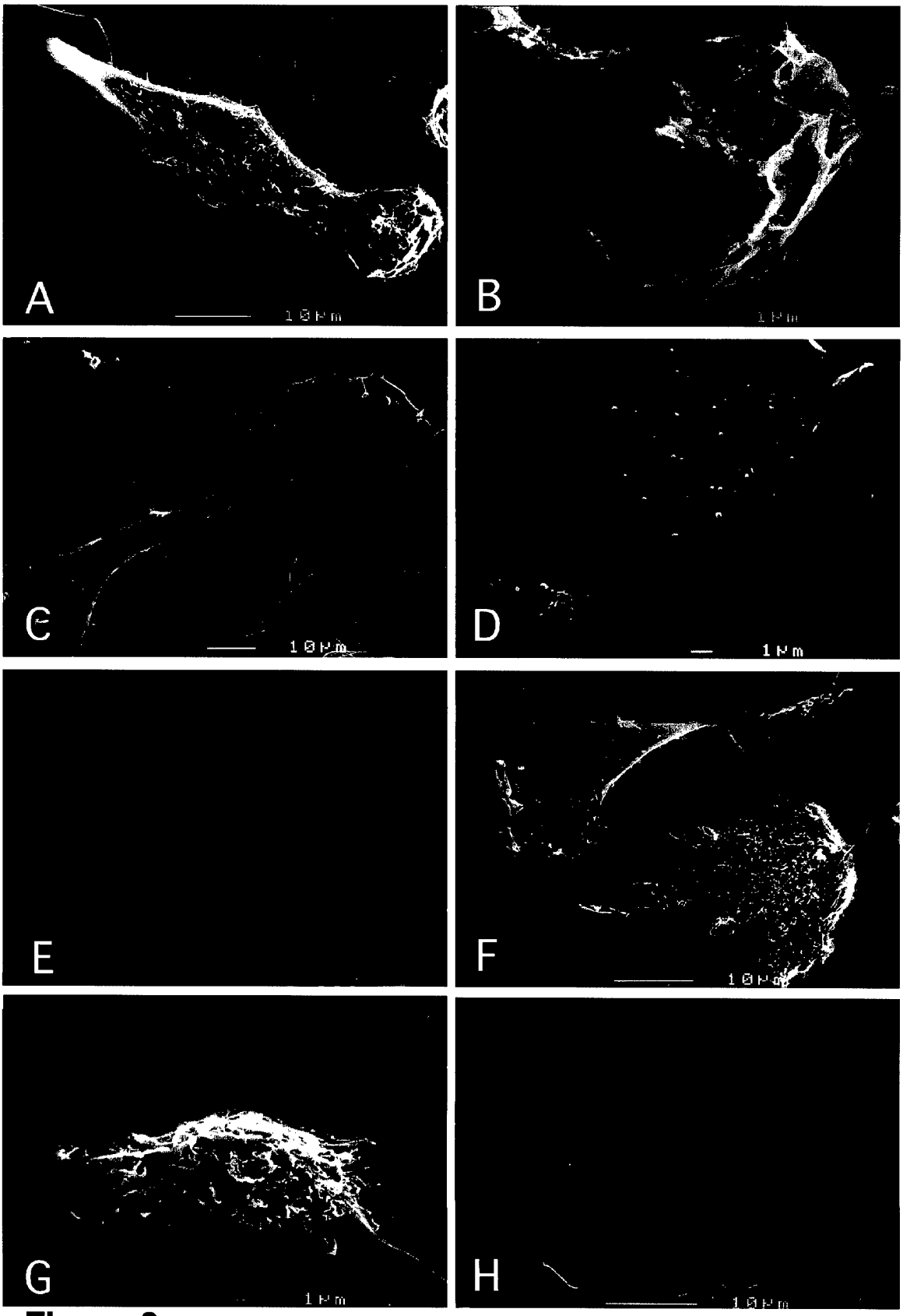

Figure 3

Figure 4

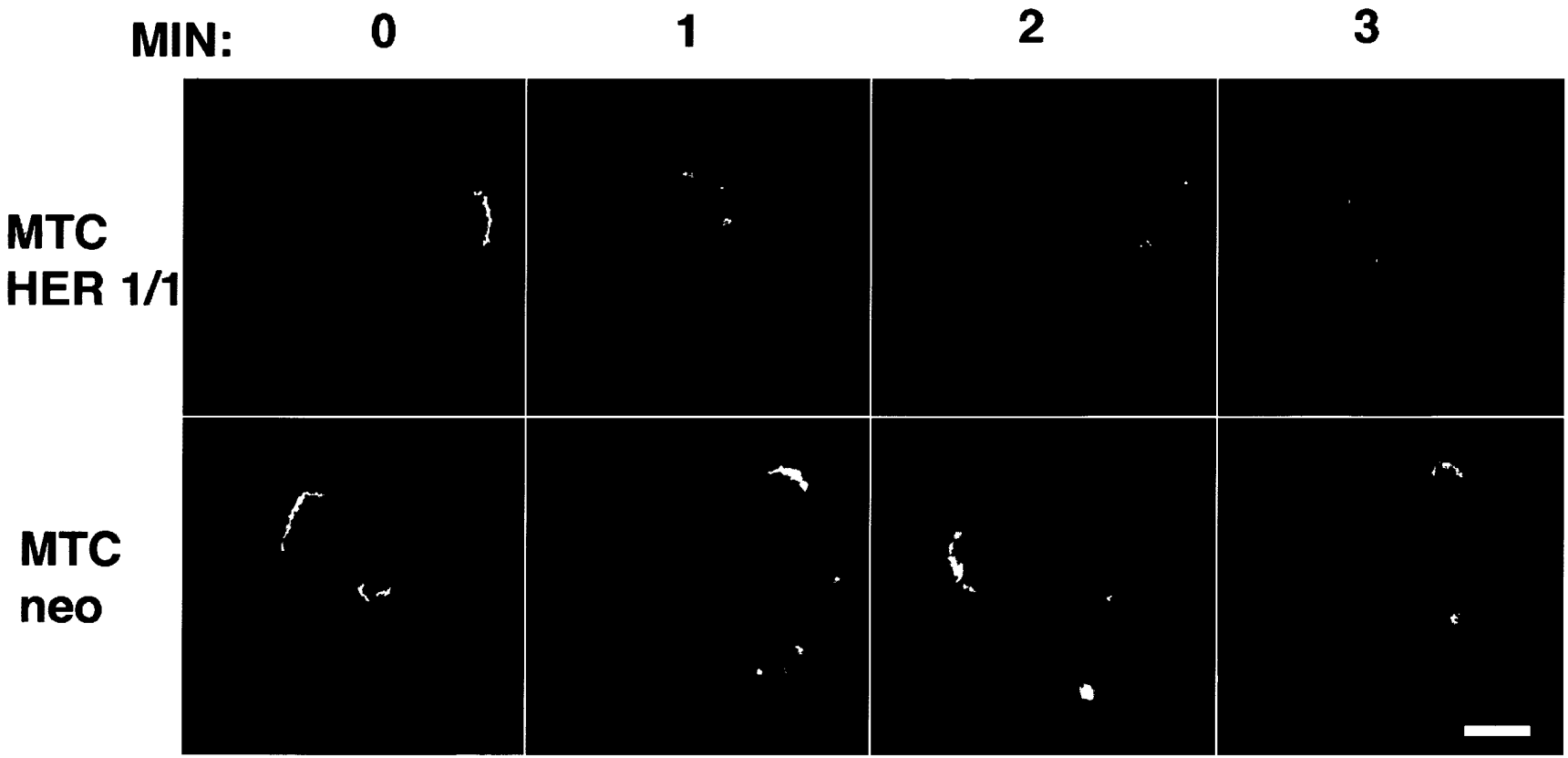

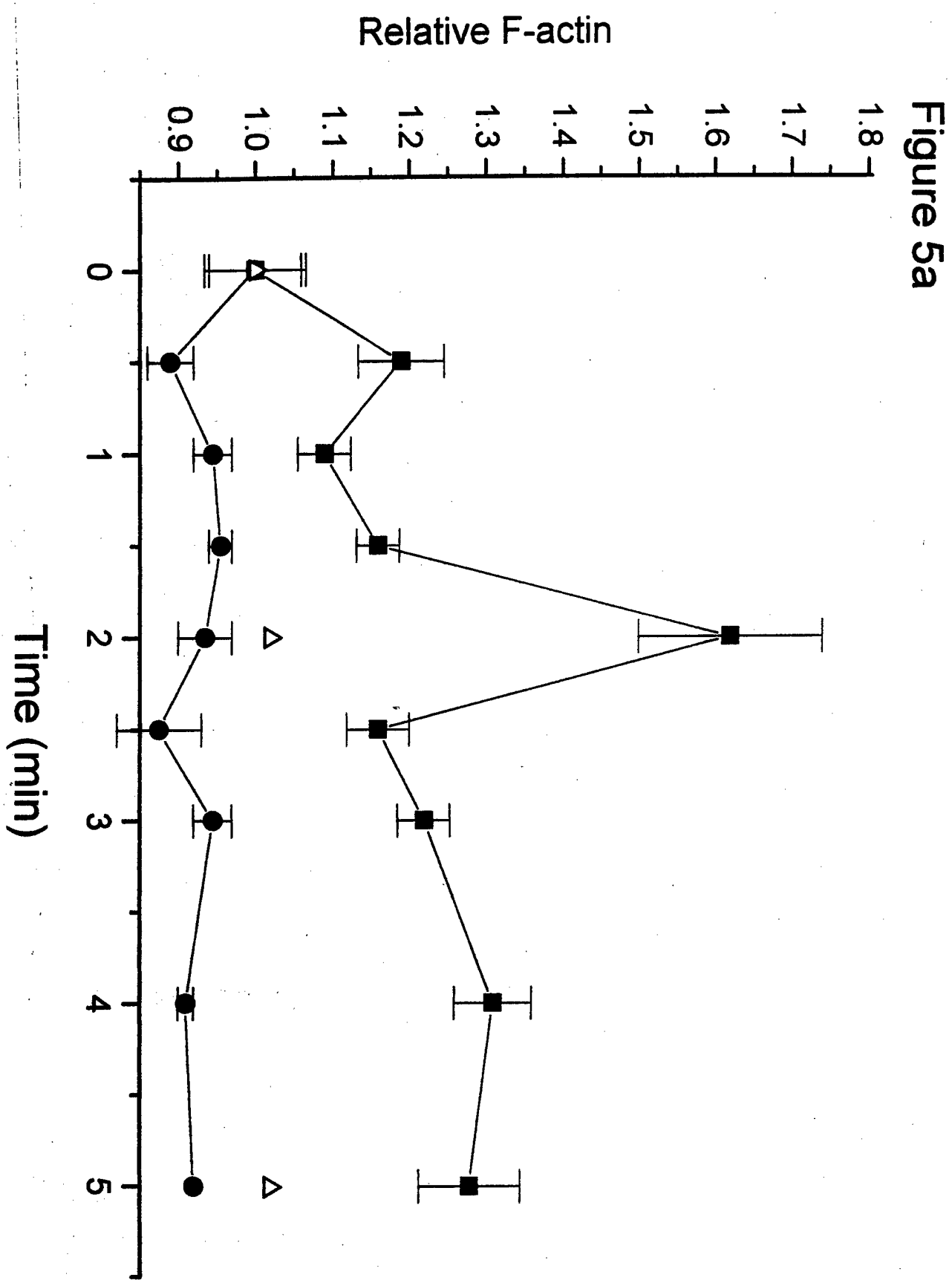

Figure 5a

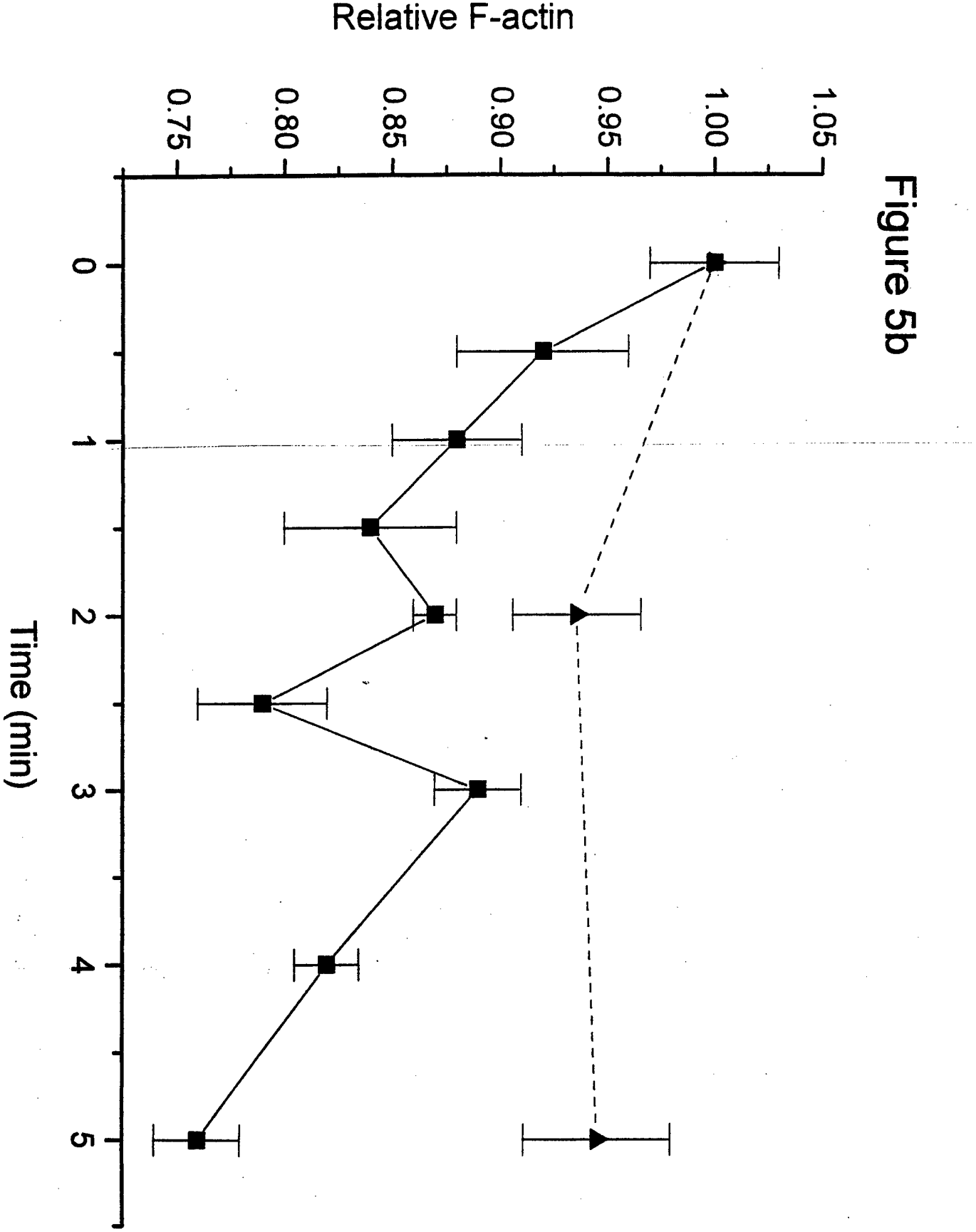

Figure 5b

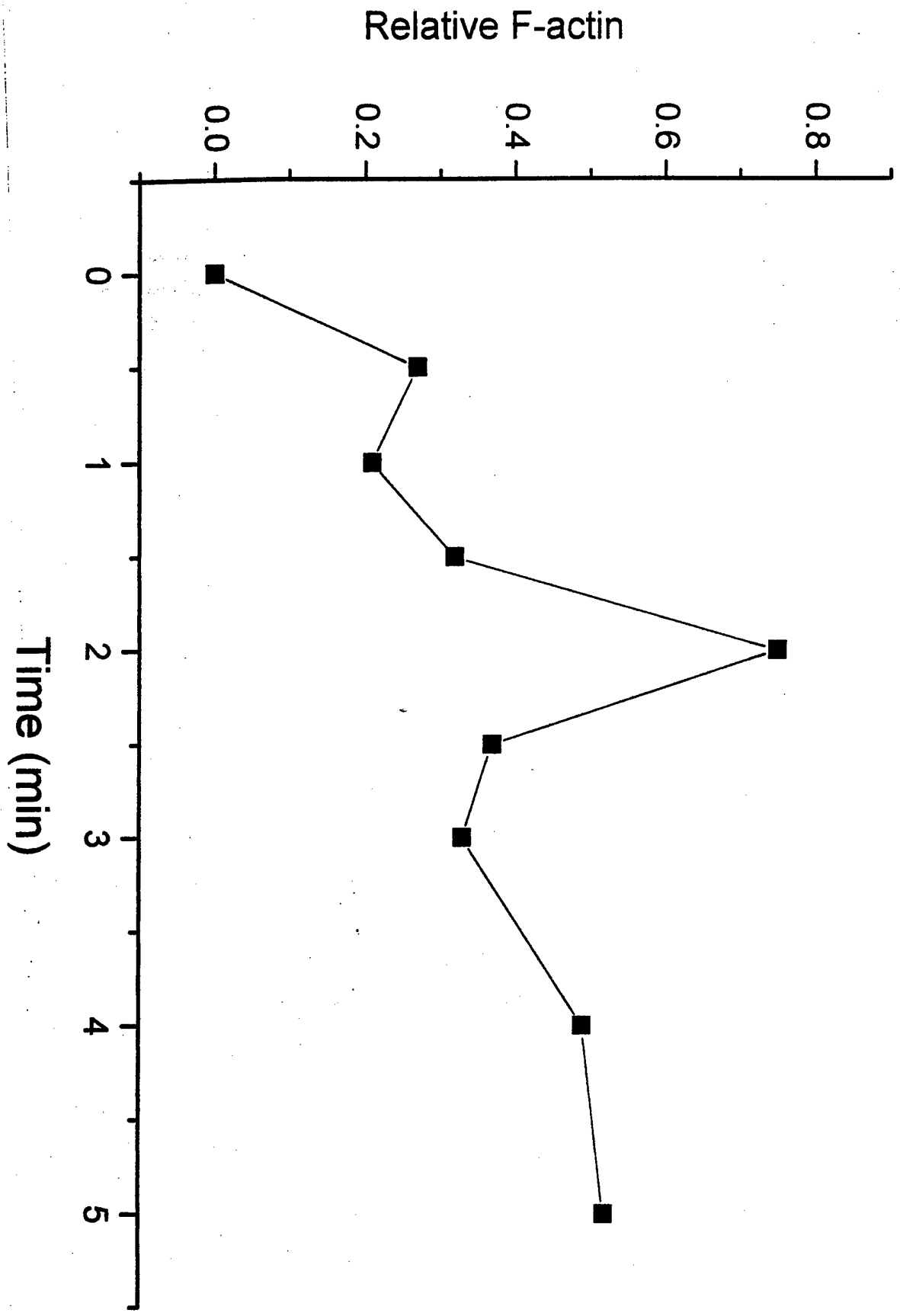

Figure 5c

Figure 6

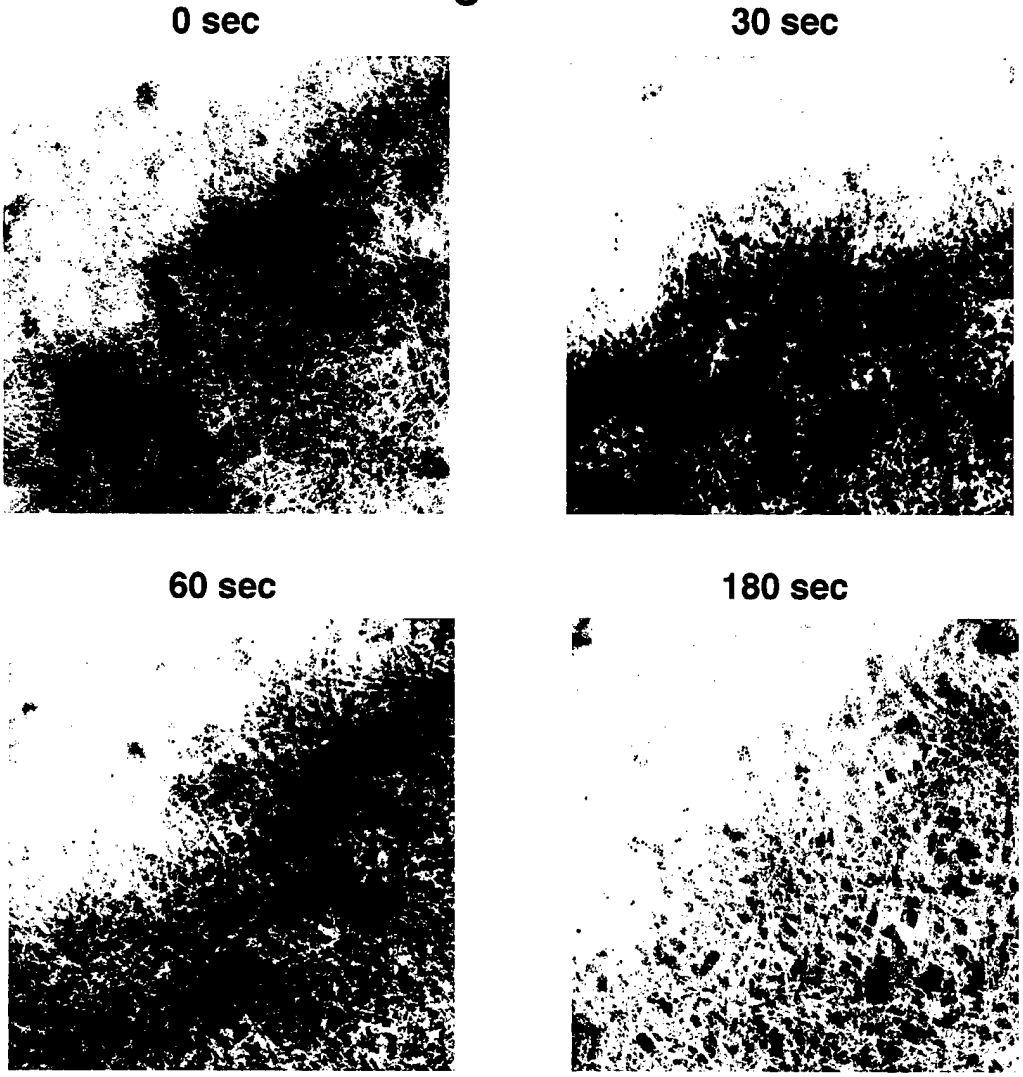

Figure 7